Unusual Nematic Liquid Crystal with Polar C_s Symmetry Formed from Aromatic Polyesters with Head−Tail Character

Masao Koike, Chu-Chun Yen, Liu Yuqing, Hitoshi Tsuchiya, Masatoshi Tokita, Susumu Kawauchi, Hideo Takezoe, and Junji Watanabe*

Department of Organic and Polymeric Materials, Tokyo Institute of Technology, Ookayama, Meguro-ku, Tokyo 152-8552, Japan

Received November 14, 2006; Revised Manuscript Received February 7, 2007

ABSTRACT: We performed second harmonic generation (SHG) measurements in the nematic liquid crystal formed from polar aromatic polyester which comprises 4-hydroxybenzoic acid and 6-hydroxy-2-naphthoic acid in a molar ratio of 73/27. The polymer is commercially available and called Vectra. The shear-oriented nematic liquid crystal of Vectra shows strong SHG mostly along the *n*-director. Since no electric poling is made, the observed SHG activity indicates that the polar ordering is spontaneously formed in the nematic liquid crystal. From detailed analyses of the SHG intensity profiles measured with combinations of polarizer and analyzer directions to the *n*-director, the nematic liquid crystal is found to possess the C_s packing symmetry; in other words, it is not uniaxial but biaxial, and the polarization arises in the symmetry plane. To search the origin of the spontaneous polarization, we prepared a series of Vectra polymer with various degrees of polymerization (DP) and two chemically modified Vectras. Of interest is that the DP of polymer significantly affects the polar structure. When DP is decreased, the SHG activity in the nematic liquid crystal disappears completely. Since the dipole moment increases with DP, the huge dipole moment of polymer is considered to be responsible for the polar ordering. In one of the two chemically modified Vectras, terephthalic acid (TA) and biphenol (BP) in an equimolar content are introduced. As expected from the dissipation of head−tail character in constituent polymer, the nematic liquid crystals lose completely the SHG activity only with an incorporation of 5 mol % of TA and BP. In another modified Vectra including 3-hydroxybenzoic acid (*m*-HBA), the head−tail character is not lost, but their liquid crystallinity is destabilized because of kink conformation induced by the *m*-HBA unit. In this system, the SHG is invariably observed for the nematic liquid crystals, but as one of the significant effects, polar biaxial nematic liquid crystal of Vectra is altered to the polar uniaxial one by the introduction of *m*-HBA above 5 mol %.

1. Introduction

Ferroelectric or polar ordering of molecules in liquid crystals is of considerable theoretical and technological interest.[1] It has been achieved in chiral and tilted smectic phases; the chirality of molecules and their tilted association into the smectic layer, which can reduce the overall symmetry of liquid crystal structure, are essential for their preparation.[2,3]

Recently, the great attention has been directed to the nonchiral ferroelectric system. Watanabe et al.[4,5] have proposed that the ferroelectric smectic phase with C_{2v} symmetry can be formed from main-chain liquid crystal polymers if two types of odd-numbered aliphatic spacers are incorporated into the backbone in a regularly alternate fashion and are segregated into different microdomains. Although the preparation of ferroelectric liquid crystal in this case failed because of the difficulty in polymer synthesis, the successful progress has been made by treating the banana-shaped molecules and bent dimer molecules.[6−12] In these exotic molecular systems, the ferroelectric and antiferroelectric responses were well identified in a relation to their characteristic packing structures. Bustamante et al.[13,14] have also reported the antiferroelctric smectic phase in certain mixtures of nonchiral side-chain polymers and their monomers as observed by pyroelectric and piezoelectric measurements.

The examples mentioned above are so-called improper ferroelectric liquid crystals, which emerge because of the introduction of chirality and the packing of polar bent-core molecules. Another approach to obtain the ferroelectric liquid crystals is based on the idea of proper ferroelectricity, which is realized by dipole−dipole interaction.[15,16] This idea has been suggested by the computer simulation and theoretical calculation. These demonstrate that ferroelectricity appears even in the nematic phase if the constituent rodlike molecules have a large dipole moment.[17−22] By considering the dipole−dipole interaction and hard-core repulsion using a simple mean-field model within the Onsager formalism, Lee et al.[19,20] presented the phase diagram where the rodlike molecules exhibit conventional isotropic−nematic, nematic−ferroelectric nematic, and direct isotropic−ferroelectric nematic transitions as a function of temperature or pressure. Park et al.[22] discussed the same phase transition behavior in the context of the phenomenological theory. It is also worth noting that the isotropic−polar biaxial nematic phase transition in biaxial molecular systems has been discussed at the phenomenological and molecular levels, suggesting interesting transition behaviors.[23]

These interesting predictions can be experimentally examined using the liquid crystalline aromatic polyesters which assume the rodlike conformation and simultaneously have the large dipole moment along the chain as a result of accumulation of dipole moment of repeating unit. Typical monomer units are 4-*p*-hydroxylbenzoic acid (*p*-HBA) and 6-hydroxyl-2-naphthoic acid (HNA). At this aspect, interesting is the X-ray analysis by Coulter et al.[24] for the crystal of aromatic polyester based on *p*-HBA. It shows that the polar polymers are packed with a net chain directionality in the crystalline phase. The polar crystal phases in a related polyester, Vectra comprising HBA and HNA, have also been suggested by second harmonic generation (SHG) measurements by Stuetz[25] and Asada.[26] Although these experimental studies have been done for the solid state, it is strongly

* Corresponding author. E-mail: jwatanab@polymer.titech.ac.jp.

10.1021/ma0626214 CCC: $37.00
Published on Web 03/08/2007

Table 1. Characterization of Vectra Polyester with Different Molecular Weights

sample	η_{inh}/dL g^{-1}	T_m/°C	rel SHG int	DP[a]
P-1	0.25	210	0.00	15
P-2	0.46	222	0.00	20
P-3	0.92	250	0.01	30
P-4	1.38	265	0.18	35
P-5	1.61	274	0.04	40
P-6	1.81	275	0.30	45
P-7	2.22	275	0.33	50
P-8	2.52	276	0.58	55
P-9	2.79	277	0.61	60
P-10	3.10	278	1.10	80
P-11	3.15	279	1.00	100
Vectra-Std	4.17	283	1.00	

[a] Degree of polymerization calculated from the molar fraction of end-capping PBA.

suggested that the polar ordering has been already formed in the nematic liquid crystals preceding the crystalline phase. In fact, we have observed strong SHG in the nematic liquid crystal formed on a process of polycondensation reaction of Vetcra.[27]

In this study, we examine more detailed polar structure in the nematic liquid crystals of Vectra and related polyesters through SHG observation. The results indicate that the nematic liquid crystal of Vectra has a specific C_s packing symmetry; that is, it is biaxial, and the polarity arises along both director axes. We further show how the molecular weight of Vectra and chemical modifications to Vectra affect the polar biaxial structure and then discuss about the key source for a specific formation of polar biaxial nematic liquid crystal.

2. Experimental Section

2.1. Synthesis of Polymer. The polymers used are aromatic copolyesters which basically comprise *p*-HBA and HNA units in a molar ratio of 73/27 shown below.

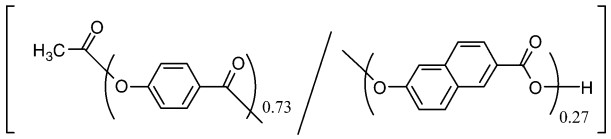

"**Vectra**"

This type of copolyester is called "Vectra", which is commercially available. The high molecular weight Vectra as a standard polymer (so named Vectra-Std) was prepared by the ester exchange reaction between acetoxyaryl groups and carboxylic acid groups in melt state at high temperatures described below.

Two monomers, 4-acetoxybenzoic acid (ABA) and 6-acetoxy-2-naphthoic acid (ANA) in a molar ratio of 73/27, were put into a glass vessel equipped with mechanical stirrer, condenser, and nitrogen inlet and outlet. The glass vessel was first heated to 250 °C under a gentle flow of nitrogen at a heating speed of 2 °C/min. After the reaction for 30−60 min at this temperature, the resulting acetic acids were removed gently and then heated again to 320 °C at 1 °C/min. Finally, the vacuum (less than 4 mmHg) was applied for an additional hour. The resulting polymer is not soluble in conventional solvents such as chloroform and tetrahydrofuran, but in specific solvents like pentafluorophenol (PFP) and hexafluoroisopropanol. The inherent viscosity was measured in a solution of PFP at a concentration of 0.5 g/dL at 40 °C. The inherent viscosity of Vectra-Std is 4.17 dL/g, as listed in the last row of Table 1, which is similar to that of the commercially available Vectra.

To prepare a homologous series of polymer with various molecular weights, we performed the polymerization by adding monofunctional phenylbenzoic acid (PBA) as an end-capping compound. The molar percents of PBA to the (ABA/ANA) mixture were changed from 1 to 6.7%, resulting in the degrees of polymerization (DP) ranging from 100 to 15. All of the polymers with their inherent viscosities, melting temperature, relative SHG intensity, and calculated DP from the content of end-capping PBA are listed in Table 1. Here, the samples are abbreviated as **P-*n***, where ***n*** is the sample number. Figure 1 shows the double-logarithmic plot of inherent viscosity vs DP. The data points for DP lower than 60 are fitted accurately by a straight line with a slope of 1.8, whereas those for higher DP follow a bent curve. The slope of 1.8 can be expected for the rigid-rod system,[28] showing that the polymerization properly proceeds as expected from the content of end-capping agent.

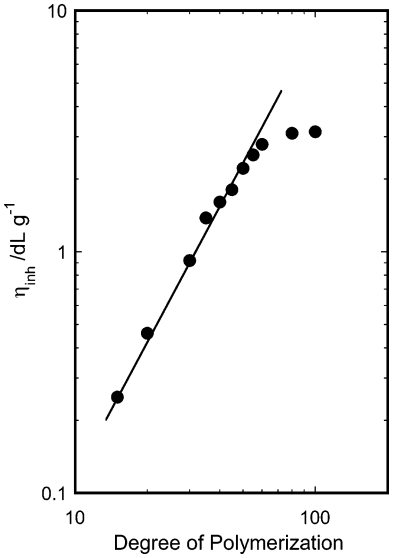

Figure 1. Double-logarithmic plot of inherent viscosity vs degree of polymerization in a series of **P-*n*** polyesters.

As a second series of polymer, we prepared the polymers including the biphenol (BP) and terephthalic acid (TA) units. Since these two units have the same functional group in para positions, the resulting polymers may lose the head−tail character. In order to properly perform the polymerization, the contents of BP and TA should be equimolar, and their contents were varied from 0 to 30%. In a third series of polymers, 3-*m*-hydroxybenzoic acid (*m*-HBA) which works as a kink unit was introduced to Vectra. The content of *m*-HBA was ranged from 0 to 100%. The inherent viscosities of the second and third series of polymer are around 4 dL/g, which is comparable to that of Vectra-Std.

2.2. Method. SHG was used as a probe to monitor the spontaneous polarization in the medium.[29] Q-switched Nd:YAG laser light (1064 nm) was incident perpendicular to the films (illumination area; 0.1 mm in diameter) after passing through a quarter-wave plate and a polarizer. SH light (532 nm) generated from the sample was detected by a Hamamatsu model-R955 photomultiplier tube in a transmitted direction after passing through an IR cut filter, an interference filter, and an analyzer. The SH light intensity was measured as a function of the rotation angle of the polarizer or analyzer.

Differential scanning calorimetric (DSC) measurements were carried out with a Perkin-Elmer Pyris-1 at a scanning rate of 10 °C/min. Wide-angle X-ray diffraction measurements were performed by using a Rigaku-Denki RU-200BH X-ray generator with Ni-filtered Cu Kα radiation. Polarized optical microscopic (POM) observations were carried out using Olympus BX50. Temperature of sample was controlled within 1 °C by using a Mettler FP82HT hot stage.

3. Results and Discussion

3.1. Huge Dipole Moment along Chain Due to Head−Tail Character of Vectra Polymer. It is known that the Vectra

Table 2. Dipole Moments (μ) and Hyperpolarizabilities (β) Calculated for *p*-HBA and *m*-HBA Oligomers at B3LYP/6-31G*

	μ/D	$\beta/10^{-30}$ esu
p-HBA ($n = 1$)	1.846	3.143
dimer ($n = 2$)	4.157	9.096
trimer ($n = 3$)	6.486	16.402
tetramer ($n = 4$)	8.835	24.411
m-HBA[a]	0.638−3.197	0.024−1.719
dimer ($n = 2$)[a]	1.440−2.311	0.501−3.506
trimer ($n = 3$)[a]	1.564−3.501	3.113−5.116
p-nitroaniline[b]	7.121	6.798

[a] There are several conformations with similar minimum energies which give different values of μ and β. [b] Listed as a typical compound.

polymer assumes rigid-rod-like conformation like other aromatic polyesters.[30−32] The most important feature of Vectra polyester which is completely different from others is that the component *p*-HBA and HNA units possess electron-donating and electron-withdrawing groups at the opposite ends. By this reason, the Vectra polyester has a polarization along its long axis as far as it sustains a rigidlike conformation.

In Table 2, the dipole moments are elucidated for the monomer, dimer, trimer, and tetramer of *p*-HBA (the main comonomer unit of Vectra):[33,34]

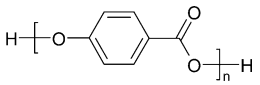

Here, the calculations were performed according to density functional theory (DFT) calculations by using the Gaussian 03 program.[35] The geometry was fully optimized at the Becke's three-parameter hybrid DFT method[36] with the Lee−Yang−Parr correlation functional (B3LYP)[37] by using the standard polarized split-valence basis set (6-31G*).[38] Then, the tensor components of the static molecular hyperpolarizability β values were obtained at the same level (B3LYP/6-31G*). The absolute value of β was estimated from the tensor components projected on the net dipole moment, β, as follows:[39]

$$\beta = \frac{3}{5}\sum_i |\beta_i \mu_i|/|\mu|; \quad i = x, y, z \tag{1}$$

Assuming the Kleinman relations,[40] it follows

$$\beta_i = \sum_j \beta_{ijj}; \quad i = x, y, z \tag{2}$$

Calculated values of μ and β are listed in Table 2. As expected, the largest component of molecular dipole moment is found to be parallel to the chain direction, and it increases in a proportion to the number of monomer units. The average increment per unit is about 2 D so that the polymer with a DP of n has a dipole moment of approximately $2n$ D.

It is noteworthy that the hyperpolarizability is relatively large as well.[33] Its value approximates that of *p*-nitroaniline (refer to the last row of Table 2) and increases proportionally with the increase of n. It is thus reliable that the present polyester shows the strong SHG, which allows us to make a confident discussion on the polarity.

3.2. Polar Nematic Liquid Crystal in Vectra. a. Thermal Transition of Vectra. Vectra is known to form the nematic phase as has been identified by optical microscopy and X-ray diffraction.[27,31,32] The crystallization takes place only partially from the nematic liquid crystal. The melting temperature of crystal to the nematic liquid crystal is 283 °C for Vectra-Std (see Table 1), but no nematic-to-isotropic transition was observed up to the decomposition temperature of around 350 °C.

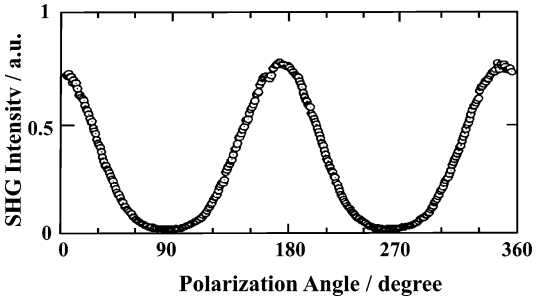

Figure 2. Dependence of the SH intensity on the polarization angle observed for the oriented film of Vectra-Std. Here, the polarization angle is defined as 0° when the polarization direction corresponds to the orientation direction of the film.

b. SH Response from Nematic Liquid Crystal of Vectra. Oriented films were prepared by shearing the nematic liquid crystal between glass substrates at 320 °C. The film thickness was about 3 μm. The order parameter of the resultant films was around 0.95 as determined by X-ray diffraction. The SH light generated from the film sample is so strong that its brilliant green color can be recognized by the naked eye. Figure 2 shows the intensity of SH light from the oriented nematic film of Vectra-Std at 290 °C as a function of input polarization direction. Here, the polarization of analyzer was fixed parallel to the orientation axis (polymer chain axis) of the nematic film, and the SHG signal was plotted against the angle between input polarization and orientation axis. Highly efficient SHG with marked anisotropy can be observed. There are maxima at around 0° and 180° and minima at around 90° and 270°, leading to the short tentative conclusion that the spontaneous polarization occurs parallel to the orientation direction. The nonlinear optical coefficient along the orientation axis has been evaluated as ∼5 pm/V using the Maker fringe method.[27]

It should be noted that we have never applied the electric field for this oriented sample. This means that the polar structure responsible for the SHG response is spontaneously formed in each domain although the neighboring domains may have the opposite direction of polarization so that the macroscopic polarity is totally cancelled out. To produce the effective SHG, the size of domain should be larger than the wavelength, and then the polar nematic structure can be regarded as a thermodynamically stable one.

c. Unusual Packing Symmetry of Polar Structure. There is a distinct point in Figure 2 which should be noted. At a first glance, Figure 2 suggests the uniaxial polar nematic liquid crystal in which the polarity arises along the *n*-director. However, one may notice by careful observation that the maximum and minimum positions are deviated from $n(\pi/2)$ positions. This small, but distinct, deviation means that the polar nematic liquid crystal has the biaxial packing symmetry. In order to clarify this point, SHG intensities were measured under various polarization conditions. Here, the laser beam was irradiated normal to the film (along the *y*-axis), and SHG intensities were plotted against the rotation angles of the polarization (Φ_p) for the fundamental beam or the polarization (Φ_a) for the SHG light. The rotation angle was defined as an angle from polymer chain axis (*z*-direction). With respect to the *z*-direction, the clockwise rotation was defined as positive when viewed along the *y*-direction, and the polar plots were made under four configurations of $\Phi_p-\Phi_a$ ($\Phi_p-0°$, $\Phi_p-90°$, $0°-\Phi_a$, and $90°-\Phi_a$). Figure 3a displays SHG profiles, $I(\Phi_p,0°)$,

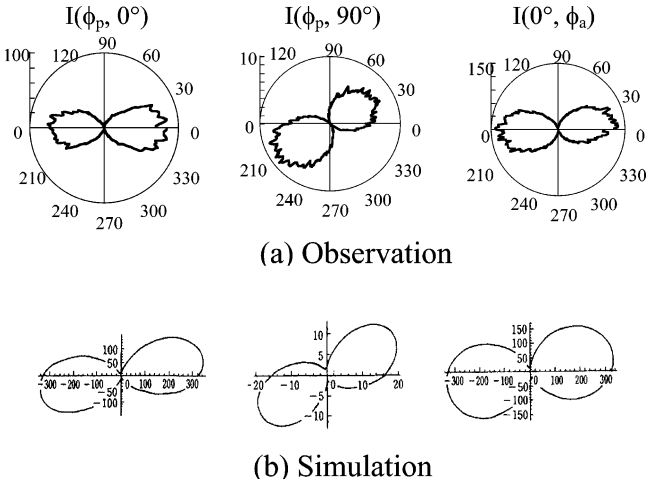

Figure 3. SHG profiles, $I(\Phi_p,0°)$, $I(\Phi_p,90°)$, and $I(0°,\Phi_a)$, (a) measured for the oriented nematic film of Vectra-Std at 300 °C and (b) simulated according to C_s symmetry (see the text). The mutual comparison of the scales of the signal intensities is effective.

$I(\Phi_p,90°)$, and $I(0°,\Phi_a)$, observed at the nematic temperature of 300 °C. $I(90°,\Phi_a)$ was too weak to detect a reasonable signal. Two following facts should be noticed. (1) All three profiles show the two-leaves pattern. (2) The intensities of SHG light show the maxima at angles deviated from 0 and 180°. These facts obviously show that the present nematic liquid crystal should not be of a simple $C_{\infty v}$ as expected for the polar uniaxial nematic liquid crystal (refer to Figure 4), but of a C_s symmetry. The χ tensor in C_s symmetry has six nonzero elements

$$\begin{pmatrix} \chi_{xxx} & \chi_{xyy} & \chi_{xzz} & 0 & \chi_{zxx} & 0 \\ 0 & 0 & 0 & \chi_{zyy} & 0 & \chi_{xyy} \\ \chi_{zxx} & \chi_{zyy} & \chi_{zzz} & 0 & \chi_{xzz} & 0 \end{pmatrix} \quad (3)$$

with an *xz* mirror plane. When the mirror plane normal makes an angle θ with respect to the light propagation direction (*y*-direction), the SHG intensity under the projection model is given by

$$\begin{aligned} I(\phi_p,\phi_a) = |(&\chi_{xxx}\sin^2\phi_p\cos^3\theta + \chi_{xyy}\sin^2\phi_p\sin^2\theta\cos\theta + \\ &\chi_{xzz}\cos^2\phi_p\cos\theta + \chi_{zxx}\sin 2\phi_p\cos^2\theta + \\ &\chi_{zyy}\sin^2\phi_p\sin^2\theta + \chi_{xyy}\sin^2\phi_p\sin 2\theta\sin\theta)\sin\phi_a + \\ &(\chi_{zxx}\sin^2\phi_p\cos^2\theta + \chi_{zyy}\sin^2\phi_p\sin^2\theta + \chi_{zzz}\cos^2\phi_p + \\ &\chi_{xzz}\sin^2\phi_p\cos\theta)\cos\phi_a|^2 \quad (4) \end{aligned}$$

It should be noted here that the oriented film has been prepared by a simple shearing. The patterns do not essentially change when the observation is made from the reverse side of the film. The fiber spun from nematic liquid crystal also gives the same result. From these reasons, the simulation can be properly done under the condition of the rotational freedom of mirror plane (i.e., θ) around the orientation axis of molecules. The simulated results are shown in Figure 3b, where the parameters used are $\chi_{xxx} = -0.07$, $\chi_{xyy} = -0.11$, $\chi_{xzz} = -0.36$, $\chi_{zxx} = 0.08$, $\chi_{zyy} = 0.10$, and $\chi_{zzz} = 1$. The agreement is very good. A large χ_{zzz} value indicates the polar ordering along the polymer chain direction, but the nonnegligible value is also detected for other χ elements.

On the other hand, the χ tensor in $C_{\infty v}$ symmetry has two nonzero elements, χ_{zzz} and χ_{zxx} ($=\chi_{zyy}$) with a C_∞ rotation around the *z*-axis. The simulated results are shown in Figure 4, where the ratio of χ_{zzz}/χ_{zxx} was assumed as 3.5. The difference from

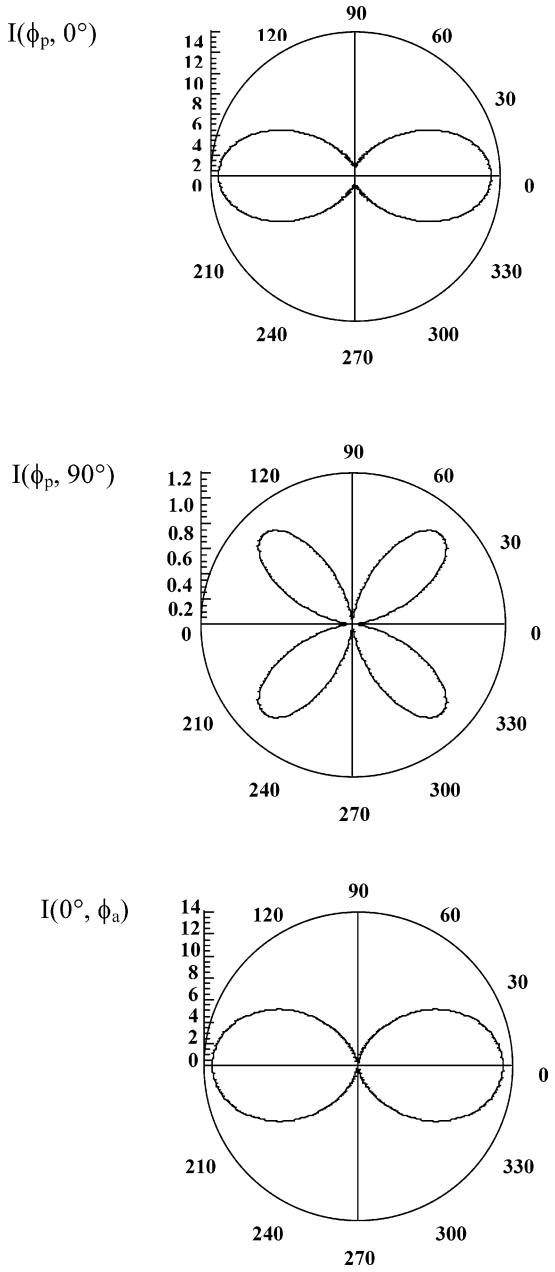

Figure 4. SHG profiles, $I(\Phi_p,0°)$, $I(\Phi_p,90°)$, and $I(0°,\Phi_a)$, simulated according to $C_{\infty v}$ symmetry (see the text).

the C_s symmetry is obvious. The four-leaves pattern is observed in the $I(\Phi_p,90°)$ profile, and the maximum and minimum intensities in the two-leaves patterns of $I(\Phi_p,0°)$ and $I(0°,\Phi_a)$ are located exactly at angles of 0° and 90°, respectively.

As a conclusion, the present nematic liquid crystal has a specific C_s packing symmetry; i.e., it is biaxial, and the polarization exists in the symmetry plane. Such a C_s symmetric nematic phase is not absurd since its possibility has been theoretically predicted.[41,42] One polar axis is along the polymer chain axis, and another polar axis directs perpendicular to the polymer chain axis. Figure 5a,b illustrates the packing structure of polymers which are schematically shown by the arrows. It should be noted that such a polar biaxial structure requires each polymer molecule to assume the specific conformation. According to the conformational analysis by DFT calculation,[34] Ph−C(=O)−O are confined on the same plane. With respect to the O−Ph bond, there are two possible conformations with lowest energy. One conformation has 60° and another has 120°

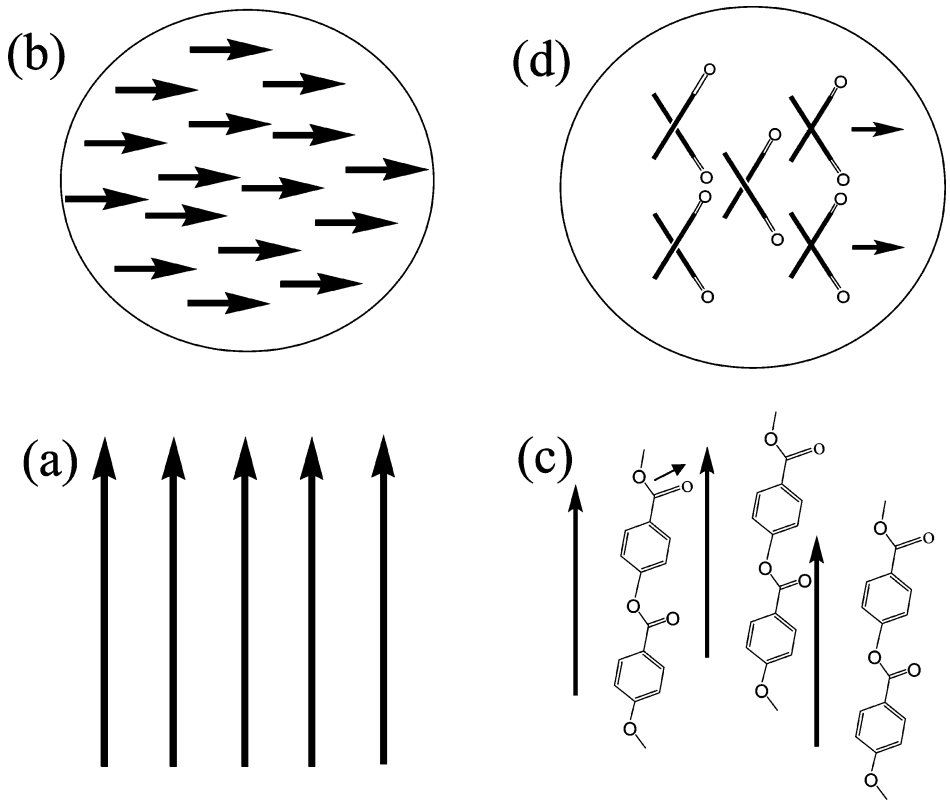

Figure 5. Illustration of polar nematic liquid crystal with C_s symmetry which satisfies the SHG data of Figure 3. The nematic liquid crystal should be biaxial, and both axes should be polar as schematically illustrated in (a) and (b). One polar axis is along the polymer chain axis as in (a), and another polar axis is directing perpendicular to the polymer chain axis as in (b). Such a polar biaxial structure requires each Vectra polymer to assume the specific conformation. (c) and (d) illustrate one of the possible conformations in which all the carbonyl groups are directed to the similar direction so that the polarization arises not only along a perpendicular direction but also in a parallel direction to the polymer chain.

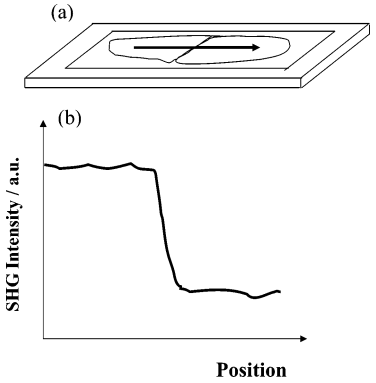

Figure 6. Measurement of relative intensity of SH light as a standard of Vectra-Std by a contact method. Here, the **P-*n*** polymer with a thickness of 10 μm was sandwiched between glass substrates and contacted with Vectra-Std, as illustrated in (a). Then, the SHG signal scattered from the surface was detected by scanning the laser beam from the area of Vectra-Std to that of the **P-*n*** polymer as shown in (b).

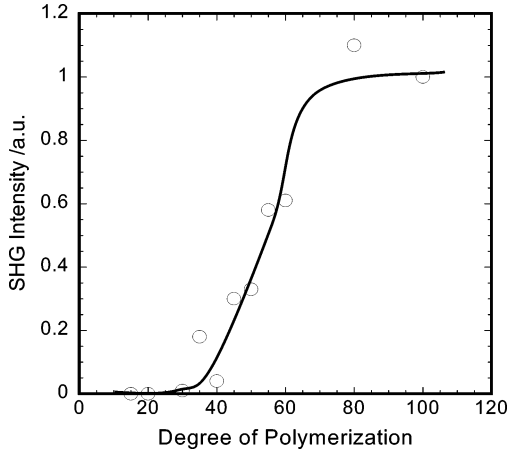

Figure 7. Variation of SH intensity with the degree of polymerization in a series of **P-*n*** polymers. Here, the relative intensities are plotted as a standard of Vectra-Std.

as an angle between the adjacent Ph−C(═O)−O planes. In Figure 5c,d, the polar packing structure is illustrated by selecting one of the possible conformations, in which all the carbonyl groups are directed to the similar direction as an average, to produce the polarization along a perpendicular direction to the polymer chain as well as in the parallel direction. Here, ones would hardly believe that such a confined conformation is sustained in fluid nematic field since the potential energy barrier around O−Ph is fairly low (less than 1 kcal/mol) so that this bond can rotate somewhat freely between two confomers.[34] Thus, we have to consider that the unusual conformational confinement would be caused by the strongly correlated dipole−dipole interaction field. Finally, it should be noted that the specific conformation of Vectra has also been suggested by NMR[43] and fluorescence data.[44]

3.3. Structural Factors of Constituent Polymer Affecting Polar Nematic Structure. Here, a question arises: what is the structural factor responsible for the formation of polar nematic liquid crystals? To clarify this point, the effects of molecular weight and chemical structures on the SHG response were examined.

a. Effect of Molecular Weight of Vectra. There are so many low-molecular-weight LC compounds with the polar conformation (or head−tail character). However, the polar nematic liquid crystals have never been reported. This means that the molecular

Chart 1

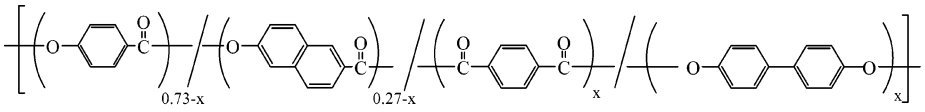

Copolyester [A]

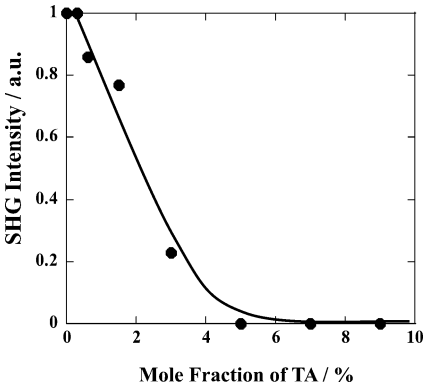

Figure 8. Variation of SH intensity with the mole fraction of TA unit in a series of copolyesters [A].

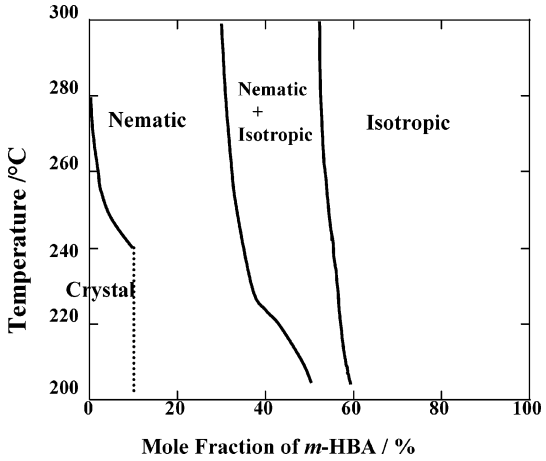

Figure 9. Phase behavior observed as a function of the mole fraction of *m*-HBA unit in a series of copolyesters [B].

weight and hence the absolute value of dipole moment are significant in the formation of polar structure.

Then, we first examined the dependence of SHG intensity on the molecular weight of Vectra polymer. Here, the relative intensities of SHG for all the **P-*n*** polymers were determined as a standard of Vectra-Std by a following contact method. The polymer with a thickness of 5−10 μm was sandwiched between glass substrates and contacted with Vectra-Std, as illustrated in Figure 6a. Then, the SH signal intensity was detected by scanning the laser beam from the area of one polymer to that of the other as observed in Figure 6b.

The relative SHG intensities of **P-1** to **P-11** are listed in the fourth column of Table 1 and plotted against the degree of polymerization (DP) in Figure 7. It is found that the SH intensity starts to increase gradually from zero at around 30, increases remarkably at 50, and then becomes constant at DP above 70. Although a change of intensity is somewhat moderate with a variation of DP probably because of the wide distribution of molecular weight, it can be concluded that the polar structure is formed only in the nematic liquid crystals of polymers with DP higher than 50. These tendencies are indeed in a qualitative agreement with the theoretical prediction that the spontaneous polarization takes place when the molecule possesses the dipole

Chart 2

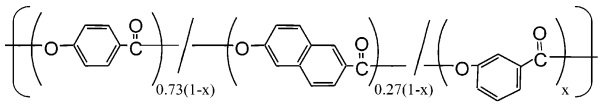

Copolyester [B]

moment exceeding the critical value.[20] The critical dipole moment in this system is around 100 D.

b. Effect of Chemical Modifications to Vectra. Next, we refer to the chemically modified copolyester [A], in which the terephthalic acid (TA) and biphenol (BP) units in an equimolar content are incorporated into Vectra. The chemical structure is shown in Chart 1. One knows that the newly introduced comonomer units would eliminate the head−tail polar nature of each polymer chain so that the resulting nematic liquid crystal should lose the polarity. In practice, the trend is clearly observed in Figure 8 where the relative SHG of the nematic liquid crystals in these copolymers is presented against the content of TA (or BP). SHG intensity sharply decreases with the increasing content of TA and becomes zero only by an introduction of 4% mole fraction of TA (or BP).

In the second series of copolyesters [B], the HBA units are introduced to Vectra (see Chart 2). In this case, head−tail nature is retained, but the rodlike nature is lost because of the kink conformation of *m*-HBA when a rich amount of *m*-HBA is introduced. Figure 9 shows the phase behavior observed in the copolyesters [B]. The nematic liquid crystals are uniformly formed in copolymers with the *m*-HBA contents lower than 30 mol %, while it is totally destabilized to transform to the isotropic liquid when the content of *m*-HBA becomes more than 60%. In the polymers with intermediate contents between 30% and 60%, the nematic and isotropic phases coexist. SHG intensities measured for the nematic liquid crystals are plotted against the mole fraction of *m*-HBA in Figure 10. One can see that the SHG intensity decreases with the mole fraction of

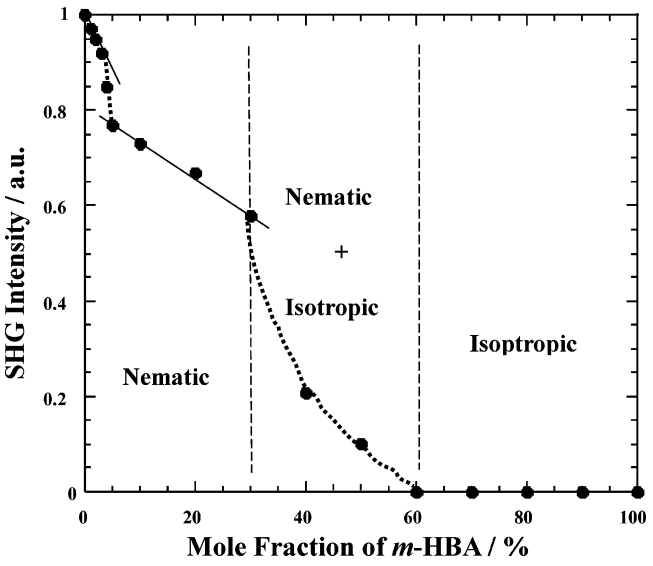

Figure 10. Variation of SH intensity with the mole fraction of *m*-HBA unit in a series of copolyesters [B].

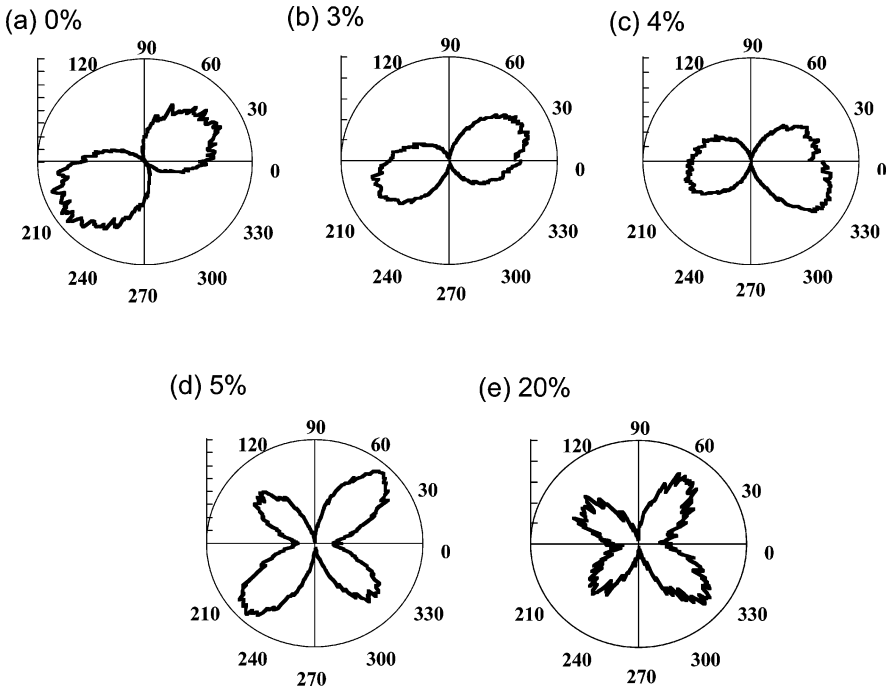

Figure 11. SHG profiles, $I(\Phi_p,90°)$, varied with mole fraction of *m*-HBA in a series of copolyesters [B].

m-HBA through four steps: the first step in a region of 0−3%, the second in a region of 4−5%, the third in a region of 5−30%, and the fourth in a region of 30−60%. It is obvious that the decrease of SHG intensity at the fourth step is caused by the decrease in the relative volume of nematic phase to the isotropic one. Besides, it is reasonable that the SHG intensity in the nematic field steadily decreases with the increase of *m*-HBA content since the hyperpolarizability of *m*-HBA is relatively smaller than that of *p*-HBA, as calculated in Table 2.

A simple question arises. Why does the SH intensity decrease steeply in a limited region of 4−5%? To clarify this point, the packing symmetry was examined for oriented nematic liquid crystal by measuring the dependences of SH intensity on polarizer and analyzer angles as in Figure 2. Figure 11 shows the content dependence of $I(\Phi_p,90°)$ profiles observed for the copolyesters with the *m*-HBA contents of 0−20%. One can find the two-leaves pattern is altered to the four-leaves pattern when the mole fraction of *m*-HBA is increased from 3 to 5%. This means that the C_s symmetry is altered to the $C_{\infty v}$; in other words, the polar biaxial nematic liquid crystal is altered to the polar uniaxial one (refer to the simulation results of Figures 3b and 4). The remarkable reduction of SHG at the second step is thus attributable to the loss of the polarization in one of the axes. Possibly, the conformational disordering enhanced by *m*-HBA kink unit may overcome the strongly correlated field which forces the *p*-HBA and HNA chains to assume the unusually confined conformation with the polarization perpendicular to the chain axis.

4. Concluding Remarks

In conclusion, the aromatic polyester discussed here forms a novel nematic liquid crystal with polar ordering along the nematic director. The SHG profiles as a function of incident or SHG polarizations are well simulated according to the model of C_s symmetry with its mirror plane rotationally disordered around the nematic director.

The polar nematic liquid crystal is formed only when the DP of polymer is higher than 50. In other words, the polar structure is preferentially formed from the polymers with the larger dipole moment than 100 D. These experimental results are consistent with the theoretical prediction,[19,20] saying that rigid-rod macromolecules with a large dipole along the rod axis have possibility to form the ferroelectric liquid crystal in a spontaneous process. On this point, it should be noted that α-helical polypeptide, another typical polymer with polar head−tail character, has also been found to form spontaneously the polar structure in their thermotropic and lyotropic cholesteric liquid crystals.[44−47]

SHG activity is lost by the chemical modification to cancel the head−tail character of Vectra. Further, introduction of kink conformation alters the C_s symmetry to the $C_{\infty v}$ one. These effects obviously show that the polar C_s symmetry determined by SHG profiles is not of artificial.

The C_s symmetry is very significant since it requires the nematic liquid crystal of Vectra to possess the biaxiality. Generally, the biaxial nematic liquid crystal is expected for the board-shaped molecules.[48−53] In addition, the C_s symmetry requires another significant conformational constraint for each polymer chain; the polymer must take up a type of conformation which produces the polarization perpendicular to the chain axis. These two requirements are satisfied if the ester carbonyl groups are sticking out to similar direction as an average as illustrated in Figure 5c,d although at a general sense, such a peculiar conformation of aromatic polyesters is hardly accepted in a fluid field. This unusual conformational constraint suggests that the strongly correlated dipole−dipole interaction field may act not only in the parallel direction to the polymer chain but also in the perpendicular one.[23]

Finally, it should be noted that we have never succeeded to obtain the macroscopically oriented polarization over the sample, which is the direct proof of the spontaneous polarization. The nematic liquid crystals cannot respond to the applied electric field since the polymeric nematic liquid crystal is highly viscous. Especially, the viscosity of the nematic Vectra is extremely high probably due to the biaxiality. As a future object, thus, we are now preparing the polar polymeric nematics which have low viscosity and are switchable upon applying the electric field.

References and Notes

(1) Goodby, J. W. In *Ferroelectric Liquid Crystals*; Gordon and Breach Press: Philadelphia, 1991.
(2) Mayer, R. B.; Liebert, L.; Strzelecki, L.; Keller, P. *J. Phys. (Paris)* **1975**, *36*, L69.
(3) Mayer, R. B. *Mol. Cryst. Liq. Cryst.* **1977**, *40*, 33.
(4) Watanabe, J.; Nakata, Y.; Simizu, K. *J. Phys. II* **1994**, *4*, 581.
(5) Watanabe, J.; Nakata, Y. *Polym. J.* **1997**, *29*, 193.
(6) Niori, T.; Sekine, T.; Watanabe, J.; Furukawa, T.; Takezoe, H. *J. Mater. Chem.* **1996**, *6*, 1231.
(7) Niori, T.; Sekine, T.; Furukawa, T.; Takezoe, H.; Watanabe, J. *Mol. Cryst. Liq. Cryst.* **1997**, *301*, 337.
(8) Sekine, T.; Watanabe, J.; Takanishi, Y.; Niori, T.; Takezoe, H. *Jpn. J. Appl. Phys.* **1997**, *6*, L1201.
(9) Niori, T.; Watanabe, J.; Choi, S. W.; Takanishi, Y.; Takezoe, H. *Jpn. J. Appl. Phys.* **1998**, *37*, L401.
(10) Izumi, T.; Kang, S.; Niori, T.; Takanishi, Y.; Takezoe, H.; Watanabe, J. *Jpn. J. Appl. Phys.* **2006**, *45*, 1506.
(11) Izumi, T.; Naitoh, T.; Shimbo, Y.; Takanishi, Y.: Takezoe, H.; Watanabe, J. *J. Phys. Chem. B* **2006**, *110*, 23911.
(12) Takanishi, Y.; Toshimitsu, M.; Nakata, M.; Takada, N.; Izumi, T.; Ishikawa, K.; Takezoe, H.; Watanabe, J.; Takahashi, Y.; Iida, A. *Phys. Rev. E* **2006**, *74*, 051703.
(13) Bustamante, E. A. S.; Yablonskii, S. V.; Ostrovskii, B. I.; Beresnev, L. A.; Blinov, L. M.; Hasse, W. *Chem. Phys. Lett.* **1996**, *260*, 447.
(14) Bustamante, E. A. S.; Yablonskii, S. V.; Ostrovskii, B. I.; Beresnev, L. A.; Blinov, L. M.; Hasse, W. *Liq. Cryst.* **1996**, *21*, 829.
(15) Takezoe, H.; Watanabe, J. *Mol. Cryst. Liq. Cryst.* **1999**, *328*, 325.
(16) Blinov, L. M. *Liq. Cryst.* **1998**, *24*, 143.
(17) Palffy-Muhoray, P.; Lee, M. A.; Petschek, R. G. *Phys. Rev. Lett.* **1988**, *60*, 2303.
(18) Biscarini, F.; Zannoni, C.; Chiccoli, C.; Pasini, P. *Mol. Phys.* **1991**, *73*, 439.
(19) Lee, J.; Lee, S.-D. *Mol. Cryst. Liq. Cryst.* **1994**, *254*, 395.
(20) Yu, C.-J.; Yu, M.; Lee, S.-D. *Jpn. J. Appl. Phys.* **2002**, *41*, L102−L104.
(21) Terentjev, E. M.; Osipov, M. A.; Sluckin, T. J. *J. Phys. A: Math. Gen.* **1994**, *27*, 7047.
(22) Park, B.; Wu, J. W.; Takezoe, H. *Phys. Rev. E* **2001**, *63*, 21707.
(23) Mettout, B.; Toledano, P.; Takezoe, H.; Watanabe, J. *Phys. Rev. E* **2002**, *66*, 031701-1.
(24) Coulter, P. D.; Hanna, S.; Windle, A. H. *Liq. Cryst.* **1989**, *5*, 1603.
(25) Stuetz, D. E. U.S. Patent 4 624 872, 1986.
(26) Asada, T. *Mol. Cryst. Liq. Cryst.* **1994**, *254*, 125.
(27) Watanabe, T.; Miyata, S.; Furukawa, T.; Takezoe, H.; Nishi, T.; Migita, A.; Sone, M.; Watanabe, J. *Jpn. J. Appl. Phys.* **1996**, *35*, L505.
(28) Yanaki, T.; Norisue, T.; Fujita, H. *Macromolecules* **1980**, *13*, 1462.
(29) Shen, Y. R. In *The Principles of Nonlinear Optics*; John Wiley & Sons: New York, 1984.
(30) Hummel, J. P.; Flory, P. J. *Macromolecules* **1980**, *13*, 479.
(31) Coulter, P.; Windle, A. H. *Macromolecules* **1989**, *22*, 1129.
(32) Jin, J.-I.; Antoun, S.; Ober, C.; W. Lenz, R. *Br. Polym. J.* **1980**, *12*, 132.
(33) Imase, T.; Kawauchi, S.; Watanabe, J. *Mol. Cryst. Liq. Cryst.* **2000**, *346*, 107; *Nonlinear Opt.* **2000**, *26*, 91.
(34) Imase, T.; Kawauchi, S.; Watanabe, J. *Macromol. Theory Simul.* **2001**, *10*, 434; *J. Mol. Struct.* **2001**, *560*, 275.
(35) Frisch, M. J.; Trucks, G. W.; Schlegel, H. B.; Scuseria, G. E.; Robb, M. A.; Cheeseman, J. R.; Montgomery, J. A.; Vreven, Jr., T.; Kudin, K. N.; Burant, J. C.; Millam, J. M.; Iyengar, S. S.; Tomasi, J.; Barone, V.; Mennucci, B.; Cossi, M.; Scalmani, G.; Rega, N.; Petersson, G. A.; Nakatsuji, H.; Hada, M.; Ehara, M.; Toyota, K.; Fukuda, R.; Hasegawa, J.; Ishida, M.; Nakajima, T.; Honda, Y.; Kitao, O.; Nakai, H.; Klene, M.; Li, X.; Knox, J. E.; Hratchian, H. P.; Cross, J. B.; Adamo, C.; Jaramillo, J.; Gomperts, R.; Stratmann, R. E.; Yazyev, O.; Austin, A. J.; Cammi, R.; Pomelli, C.; Ochterski, J. W.; Ayala, P. Y.; Morokuma, K.; Voth, G. A.; Salvador, P.; Dannenberg, J. J.; Zakrzewski, V. G.; Dapprich, S.; Daniels, A. D.; Strain, M. C.; Farkas, O.; Malick, D. K.; Rabuck, A. D.; Raghavachari, K.; Foresman, J. B.; Ortiz, J. V.; Cui, Q.; Baboul, A. G.; Clifford, S.; Cioslowski, J.; Stefanov, B. B.; Liu, G.; Liashenko, A.; Piskorz, P.; Komaromi, I.; Martin, R. L.; Fox, D. J.; Keith, T.; Al-Laham, M. A.; Peng, C. Y.; Nanayakkara, A.; Challacombe, M.; Gill, P. M. W.; Johnson, B.; Chen, W.; Wong, M. W.; Gonzalez, C.; Pople, J. A. *Gaussian 03*, Revision B.05; Gaussian, Inc.; Pittsburgh, PA, 2003.
(36) Becke, A. D. J. *Chem. Phys.* **1993**, *98*, 5648.
(37) Lee, C.; Yang, W.; Parr, R. G. *Phys. Rev.* **1988**, *B37*, 785.
(38) Hariharan, P. C.; Pople, J. A. *Chem. Phys. Lett.* **1972**, *66*, 217.
(39) Kurtz, H. A.; Stewart, J. J. P.; Dieter, K. M. *J. Comput. Chem.* **1990**, *11*, 82.
(40) Kleinman, D. A. *Phys. Rev.* **1962**, *126*, 1977.
(41) Brand, H. R.; Cladis, P. E.; Pleiner, H. *Int. J. Eng. Sci.* **2000**, *38*, 1099 (in this reference, C_s is called C_{1h}).
(42) Mettout, B. *Phys. Rev. E* **2006**, *74*, 041701.
(43) Kurosu, H.; Ookubo Tuchiya, H.; Ando, I.; Watanabe, J. *J. Mol. Struct.* **2001**, *574*, 153.
(44) Uchida, Y.; Huang, H. W.; Horie, K.; Qing, L. Y.; Tuchiya, H.; Watanabe, J. *J. Polym. Sci., Part B: Polym. Phys.* **2000**, *38*, 2922.
(45) Park, B.; Kinoshita, Y.; Takezoe, H.; Watanabe, J. *Jpn. J. Appl. Phys.* **1998**, *37*, L136.
(46) Watanabe, J.; Hirose, Y.; Tokita, M.; Watanabe, T.; Miyata, S. *Macromolecules* **1998**, *31*, 5937.
(47) Yen, C.-C.; Tokita, M.; Park, B.; Takezoe, H.; Watanabe, J. *Macromolecules* **2006**, *39*, 1313.
(48) Luckhurst, G. R. *Thin Solid Films* **2001**, *393*, 40.
(49) Chandrasekhar, S.; Nair, G. G.; Rao, S. D. S.; Prasad, S.; Krishna, P. K.; Blunk, D. *Liq. Cryst.* **1998**, *24*, 67.
(50) Pratibha, R.; Madhusudana, N. V.; Sadashiva, B. K. *Science* **2002**, *288*, 2184.
(51) Acharya, B. R.; Primak, A.; Dingemans, T. J.; Samulski, E. T.; Kumar, S. *Pramana* **2003**, *61*, 231.
(52) Acharya, B. R.; Primak, A.; Kumar, S. *Phys. Rev. Lett.* **2004**, *92*, 145506.
(53) Fu, K.; Sone, M.; Tokita, M.; Watanabe, J. *Polym. J.* **2006**, *38*, 1.

MA0626214